2014 IEEE International Conference on Robotics & Automation (ICRA)
Hong Kong Convention and Exhibition Center
May 31 - June 7, 2014. Hong Kong, China

An Automated System for Persistent Real-Time Truck Parking Detection and Information Dissemination*

Doug J. Cook[1], Ted Morris[2], Vassilios Morellas[3], and Nikolaos Papanikolopoulos[3]*

Abstract— **Tractor-trailer freight hauling has increased markedly within the United States over the past several years, resulting in higher truck volumes. commercial heavy vehicle drivers are required under federal Hours Of Services rules to rest and take breaks to mitigate driving while fatigued. Although there are many rest area facilities available to truck drivers, there is a lack of persistent timely information on truck parking availability. An automated real-time sensing system to directly detect and disseminate parking space occupancy from truck parking facilities is described in detail. The methodology and system architecture are presented in which robust, persistent, parking occupancy detection is achieved by extending Structure from Motion (SfM) techniques using a multiplicity of commercial, off-the-shelf cameras. The system architecture allows the approach to be scaled to a region-wide comprehensive truck parking information system for commercial heavy vehicle drivers and operators. Per parking space detection accuracy of 99% is achieved over continuous operation. Classification accuracy under diverse scene and parking behavior scenarios is discussed.**

I. INTRODUCTION

There is general acceptance among policy makers and the research community that driver fatigue increases crash risk and is a contributing factor in motor vehicle crashes ([1], [2], [3]). Driving heavy vehicles such as commercial semi-tractor trucks have received considerable attention due to their weight and size. In 2009, 3,380 people were killed in truck crashes (including 503 Commercial Motor Vehicle (CMV) drivers) and 74,000 were injured. The link between heavy vehicle fatigue and increased crash risk has led to stepped up enforcement of hours of services rules in the United States to limit allowable driving time, requiring drivers to obtain a minimum amount of rest during and between their shifts [4]. Although, there are many rest area facilities available to truck drivers, studies found truck drivers routinely complain about the difficulty of obtaining information on truck parking availability for these facilities [5].

Increasing the number of truck stops and rest areas, or adding capacity to existing ones, may be either financially intractable, or incompatible with local restrictions. Intelligent Transportation System (ITS) technologies can be used to provide real-time information that would redirect drivers to nearby facilities with available parking, thereby utilizing the existing capacity more effectively [6]. A review of proposed techniques to monitor vehicle parking capacity is presented next.

Real-time parking monitoring methodologies can be categorized as *indirect* and *direct*. *Indirect* methodologies are based on detecting and classifying vehicles at all ingress and egress points of the parking facility and summing the difference over accumulated counts at specified time intervals, as opposed to directly monitoring each parking space status. The indirect approach has been facilitated using pavement embedded wireless magnetometers ([5], [7]) or computer vision ([8]). Although ingress-egress count detection is intuitively obvious, the general problem is that small counting and vehicle classification errors accumulated over time which led to unacceptably high parking occupancy errors. For example due to non-stationary sensor bias, an approximate count error of about one vehicle per day was observed for facilities providing 27 to 35 truck parking stalls [7]. An occupancy detection accuracy of 96% was stated as the threshold for an acceptable level of accuracy [8].

There have been many proposed methodologies reported in literature to directly monitor parking spaces using camera sensors. Modi et. al [9] demonstrated a computer vision-based approach to directly detect space occupancy of vehicles utilizing a foreground/background blob segmentation algorithm based on time-variant mixture of Gaussians combined with shadow removal. Researchers in [10] orthorectified 2D camera views of vehicle parking spaces into a top-down viewpoint before segmenting each parking space. A Markov Random Field model is used to impose a penalty cost to disambiguate overlapping probabilities in adjacent parking spaces that lead to conflicting conclusions of occupancy, based on mean pixel color features compared to an apriori color feature model of empty spaces. They reported an accuracy range from 76% to 94%. True [11] computes color (in Y-CrCB space) histograms of parking space regions defined a-priori. The luminance component is discarded to mitigate intensity changes in the scene. The histograms were compared with a training set of histograms to classify the space with an accuracy between 68% and 94%. Seo & Urmson [12] utilized fly-over aerial images to train an SVM linear classifier. A classification accuracy of 91.5% was achieved in one non-training Google aerial photo. Bong et. al [13] used color subtraction from an a-priori vacant background image to obtain large difference binary blobs which were ANDed with Sobel edge detection

*The study was supported by the Minnesota Department of Transportation, and the US Department of Transportation, Federal Highway Administration Truck Parking Facilities Program, Grant #MNDOT/9908 WO 24-USDOT/TFAC8812-056, and the National Science Foundation through grants #IIP-0934327, #IIP-1032018, and #IIP-1332133.

[1]Doug Cook can be contacted at doug.j.cook@gmail.com

[2]Ted Morris, Dept. of Computer Science & Digital Technology Center, University of Minnesota, tmorris@umn.edu

[3]Vassilios Morellas, Nikolaos Papanikolopoulos, Faculty, Dept. of Computer Science, University of Minnesota, e-mail: morellas@cs.umn.edu, and npapas@cs.umn.edu

of the difference image. Shadow removal was obtained by discriminating the density of edges in a shadow vs. a vehicle. The system was not tested under various lighting conditions. In [14], a Bayesian discriminator was designed from Principal Component Analysis (PCA) using Canny edge density, variance of intensity, and pixel correlation with a background image for one private vehicle parking space. 1,687 camera images collected over 14 days were analyzed with a detection rate of 99%. Researchers in [15] computed Harr-like features within 24x24 pixel patches to discriminate between empty, and occupied spaces (from background empty space model) Thirty samples were analyzed for a region of interest of four parking spaces, with a classification accuracy between 90% and 100%.

To conclude, there are a number of challenges with such 2D image computer vision techniques arising from rapid changes in background illumination, glare, and partial occlusions from overlapping vehicles. The latter problem is especially exacerbated with commercial heavy vehicles because of their larger size and height relative to private vehicles.

II. METHODOLOGY FOR PARKING DETECTION

A. Overview

3D Reconstruction or SfM (Structure from Motion) uses a multiplicity of images from uncalibrated cameras at arbitrary positions which observe a common scene and then use features from these images to reconstruct a 3D representation of the scene. In this system, images from three cameras are combined to reconstruct the scene (Fig. 2). The nature of the 3D reconstruction can avoid the typical challenges of shadows and occlusion encountered in the aforementioned 2D approaches. Image correspondence recognizes, for instance that a shadow on the ground exists on a flat surface rather than an "edge" of some object. Likewise, occlusions are resolved by using a different point of view in 3D space where they do not interfere with object recognition. Segmentation of objects of interest from the background can then be completely unaffected by these typical 2D pitfalls. Furthermore, environmental factors such as lighting and weather do not affect classification as long as reconstruction does not fail for lack of discernible image features. For example, during rain and snow the method succeeded since falling snow (Figure 3) or rain was not reconstructed as part of the scene.

The approach is that, using the 3D reconstruction of the truck parking lot with known 3D locations of the parking lanes, the scene is transformed into real-world coordinates and then geometric techniques are used to segment and sample the 3D space above the parking space to determine if an object such as a vehicle occupies the space (Fig. 1, bottom of 2).

B. Scene Reconstruction

The methodology used in this paper is an SfM implementation that uses Bundle adjustment and Patch-based Multi-View Stereo (PMVS) [18], [19] to achieve reconstruction.

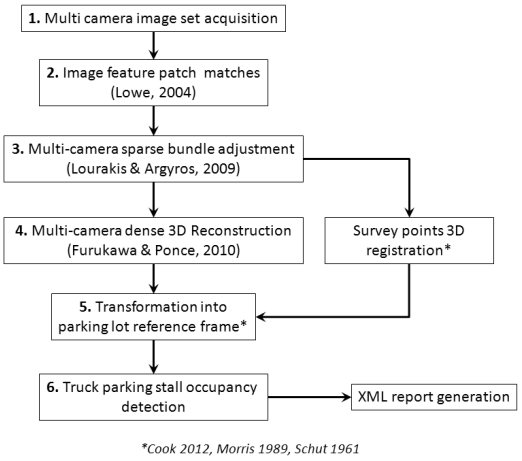

Fig. 1: Computer vision detection and classification work flow [16],[17].

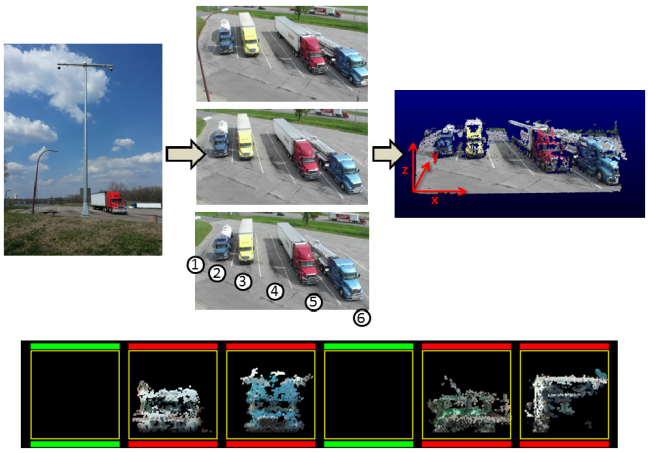

Fig. 2: Data acquisition, registration, and detection flow.

Fig. 3: Winter weather performance.

The theory and approach of this software are described briefly.

First, SIFT features [20] are collected from each image and are then matched across images to determine candidate image coordinates corresponding to commonly observed real world coordinates. These feature correspondences are used as priors for the Bundler optimization bundle adjustment procedure.

Given some camera matrix P_i for an image *i*, we let X_j represent the 3D position of a point *j* and x_{ij} to represent an estimated 2D position for that point in an image *i*. For this case the total re-projection error can be stated as:

$$\sum_{i,j} d(P_i X_j, x_{ij})^2 \tag{1}$$

where *d()* represents the image distance of the reprojected point to the location of the feature which was projected.

Minimization of this error is the goal of bundle adjustment. The minimization technique used is the Levenberg-Marquard (LM) optimization procedure. This non-linear least squares minimization is a combination of steepest descent and Gauss-Newton helps to optimize the convergence such that it converges quickly from initial guesses. EXIF data from the images is used to seed the focal length of the cameras. The end result is that the Bundler [21] estimates the intrinsic and extrinsic camera parameters and also produces a sparse reconstruction of the scene.

The camera parameters obtained from the Bundler are used to initialize the PMVS. PMVS (Patch-based Multi-view Stereo Software) is "a... algorithm for calibrated multi-view stereopsis that outputs a (quasi) dense set of rectangular patches covering the surfaces visible in the input images" [18]. The reconstruction happens through an iterative process of matching, expanding, and filtering. Patch based features are matched along epipolar lines and are considered in depth order (distance from 3D world coordinate to optical center of camera) starting with the closest. The first patch along an epipolar line that is photo-consistent in at least three images is selected. After selection, expansion occurs by adding neighbor patches that also meet a photo-consistency criteria. After expansion, filtering occurs. Expanded patches are removed if they correlate poorly, or if they seem to occur inside an object's surface, or are determined to be an outlier in terms of photo-consistency.

In this utilization of Bundler/PMVS, camera focal lengths and CCD element size were utilized as initialization parameters for the Bundler, with a large penalty weighting set for focal length as the camera calibrations indicated that focal length remained nearly constant.

The aforementioned bundled optimization solution for intrinsic and extrinsic multi-camera parameters in [21] is expressed in an arbitrary scale and world coordinate system and is affected by the initial putative matches between the captured image sets. A robust registration method is required to accurately align the (quasi) dense reconstructions with the parking spaces and surface of the lot. The procedure to do so is described next.

C. Registration and Alignment

First, the 3D end-lane and mid-lane locations, $\boldsymbol{L_i}, i = 1..m$, for each parking stall were surveyed using a DGPS system with sub-decimeter accuracy (measurements between digitized points were within 0.1 meters at 2 standard deviations in X and Y, using a local State Plane UTM projection). For 15 lanes, $m = (15+1) \times 3 = 48$ surveyed 3D coordinates. For each image set $I_n, n = 1..3$, in a time sample s is acquired, the Bundler intrinsic and extrinsic parameters are determined for each camera. Then for each camera image I_n in the set of images, image points, $\boldsymbol{p_{i,n}}$, are extracted which correspond to a visible 3D survey points L_i. The intrinsic and extrinsic solution then are used to back-project each *undistorted* 2D coordinate $\boldsymbol{p'_{i,n}}$ into its equivalent world coordinate, $\hat{\boldsymbol{L}}_{\boldsymbol{i}}$ using each camera pair, (j,k). With 3 cameras, there will be $3 \times (3-1)/2 = 3$ back projection solutions, for a given $\hat{\boldsymbol{L}}_{\boldsymbol{i}}$ with $j,k = \{\{1,2\},\{2,3\},\{1,3\}\}$. For each back projected 3D coordinate $\hat{\boldsymbol{L}}_{\boldsymbol{i}}$ a 3D back-projection error vector, $\boldsymbol{\epsilon_{i,(k,j)}}$, is computed as the difference vector orthogonal to the two closest 3D points, $\boldsymbol{\alpha_j}$, $\boldsymbol{\beta_k}$ lying on each of two normal direction rays, $\boldsymbol{u_j} = \boldsymbol{p'_{i,j}}/f_j$, $\boldsymbol{u_k} = \boldsymbol{p'_{i,k}}/f_k$ emanating from the camera pair (j,k) focal centers, $\boldsymbol{c_j}$, $\boldsymbol{c_k}$, i.e.,

$$\boldsymbol{\epsilon_{i,(k,j)}} = \boldsymbol{\alpha_j} - \boldsymbol{\beta_k} \tag{2}$$

$$\hat{\boldsymbol{L}}_{\boldsymbol{i}} = \boldsymbol{\epsilon_{i,(k,j)}}/2 + \boldsymbol{\alpha_j} \tag{3}$$

$$\text{where} \quad \boldsymbol{\alpha_j} = \boldsymbol{c_j} + a_j \cdot (\boldsymbol{u_j} - \boldsymbol{c_j})/d \tag{4}$$

$$\boldsymbol{\beta_k} = \boldsymbol{c_k} + a_k \cdot (\boldsymbol{u_k} - \boldsymbol{c_k})/d \tag{5}$$

with the scalars a_j, a_k, and d computed by:

$$a_j = (\boldsymbol{u_k} - \boldsymbol{c_k}) \times (\boldsymbol{c_j} - \boldsymbol{c_k}) \bullet (\boldsymbol{u_j} - \boldsymbol{c_j}) \times (\boldsymbol{u_k} - \boldsymbol{c_k})$$
$$a_k = (\boldsymbol{u_j} - \boldsymbol{c_j}) \times (\boldsymbol{c_j} - \boldsymbol{c_k}) \bullet (\boldsymbol{u_j} - \boldsymbol{c_j}) \times (\boldsymbol{u_k} - \boldsymbol{c_k})$$
$$d = (\boldsymbol{c_j} - \boldsymbol{c_k}) \times (\boldsymbol{u_k} - \boldsymbol{c_k}) \bullet (\boldsymbol{u_j} - \boldsymbol{c_j}) \times (\boldsymbol{u_k} - \boldsymbol{c_k}).$$

Three estimates of $\hat{\boldsymbol{L}}_{\boldsymbol{i}}$ are computed and retained: 1) the mean value between all camera pairs, 2) the minimum error $\boldsymbol{\epsilon_{i,(k,j)}}$ estimate of $\hat{\boldsymbol{L}}_{\boldsymbol{i}}$, and 3) the estimate associated with the largest projection angle the between $\boldsymbol{u_j}$ and $\boldsymbol{u_k}$. For each set of estimates, RANSAC with least-squares fit of a plane is used to eliminate outliers out-of-plane plane points. The remaining set of r back projected coordinates in the acquired time sample s are then used to estimate an optimal uniform scale factor, S_s, rotation matrix, $\boldsymbol{R_s}$, and translation vector, $\boldsymbol{t_s}$ [17],[22]. The algorithm in [17] is modified slightly by first normalizing each coordinate $\hat{\boldsymbol{L}}_{\boldsymbol{i}}$ and $\boldsymbol{L_i}$ relative to their respective point centroids:

$$\hat{\boldsymbol{l}}_{\boldsymbol{s,i}} = (\hat{\boldsymbol{L}}_{\boldsymbol{i}} - \hat{\boldsymbol{\rho}}_{\boldsymbol{s}})/\|\hat{\boldsymbol{L}}_{\boldsymbol{i}} - \hat{\boldsymbol{\rho}}_{\boldsymbol{s}}\| \tag{6a}$$

$$\boldsymbol{l_i} = (\boldsymbol{L_i} - \boldsymbol{\rho})/\|\boldsymbol{L_i} - \boldsymbol{\rho}\| \tag{6b}$$

$$\hat{\boldsymbol{\rho}}_{\boldsymbol{s}} = \frac{1}{r} \cdot \sum_{n=1}^{r} \hat{\boldsymbol{L}}_{\boldsymbol{i},n}, \qquad \boldsymbol{\rho} = \frac{1}{r} \cdot \sum_{n=1}^{r} \boldsymbol{L}_{\boldsymbol{i},n} \tag{7}$$

The normalized representations in (6), are then expressed in quaternion form, with the real component, q_0 equal to zero.

The rotation, $\hat{\boldsymbol{q}}_{\boldsymbol{R}_s}$, of the normalized coordinates $\hat{\boldsymbol{l}}_{\boldsymbol{s},\boldsymbol{i}}$ into $\boldsymbol{l_i}$ is also expressed as a quaternion through the Euler's formula, which is then augmented row-wise and solved in the least square sense, constraining $\|\hat{\boldsymbol{q}}_{\boldsymbol{R}_s}\| = 1$ (see [17] for further details of the derivation):

$$\hat{\boldsymbol{q}}_{\boldsymbol{l},\boldsymbol{s}} \times \hat{\boldsymbol{q}}_{\boldsymbol{R}_s} - \hat{\boldsymbol{q}}_{\boldsymbol{R}_s} \times \boldsymbol{q_l} = 0 \tag{8}$$

Then the uniform estimate of scale $S = \|L_i - \boldsymbol{\rho}\|/\|\hat{\boldsymbol{L}}_{\boldsymbol{i}} - \hat{\boldsymbol{\rho}}_{\boldsymbol{s}}\|$ from (6) and the translation into the reference survey coordinate system is subsequently computed by

$$\boldsymbol{t_s} = \boldsymbol{\rho} - \hat{\boldsymbol{\rho}}_{\boldsymbol{s}} \cdot S_s. \tag{9}$$

Recall that from the time sample s three separate sets of r matched points $(\hat{\boldsymbol{L}}_{\boldsymbol{i}},\ \boldsymbol{L_i})$ are used to compute their representative rotation, translation and uniform scale parameters defined in (9) and (8). A final representative set is selected based on the aforementioned transformation parameters which produce the smallest RMS error between the transformed back projected coordinates, $\hat{\boldsymbol{L}}_{\boldsymbol{i}}{}'$ and $\boldsymbol{L_i}$.

Typically, a RMS error of 0.5 meters was observed along any axis which resulted in significant detection errors. A second alignment refinement step was developed to correct for non-linear scale effects in the real-world 3D space. A first order correction in the horizontal x, y plane is estimated from the matching set, of r correspondences, $\hat{\boldsymbol{L}}_{\boldsymbol{i}}{}'$ and $\boldsymbol{L_i}$, while a second order correction model to correct elevation, ΔZ, was estimated using the dense *transformed* 3D PMVS reconstruction data:

$$\Delta X = a_0 + a_1 \cdot g_x + a_2 \cdot g_y \tag{10a}$$

$$\Delta Y = b_0 + b_1 \cdot g_x + b_2 \cdot g_y \tag{10b}$$

$$\Delta Z = c_0 + c_1 \cdot g_x + c_2 \cdot g_y + c_3 \cdot g_x \cdot g_y + c_4 \cdot g_x^2 + c_5 \cdot g_y^2 \tag{10c}$$

where $g_{()}$ in (10a) through (10c) refer to the x, y, z components of the *transformed* dense PMVS reconstruction points, $\hat{\boldsymbol{g}}_{\boldsymbol{i}}{}'$.

The elevation correction procedure searches for good candidate dense points that are representative of the parking lot surface using the following 2-step filtering method. First, an elevation boundary is placed above, and below, the plane based on the aforementioned RMS error along the vertical axis relative to the reference survey points $\hat{\boldsymbol{L}}_{\boldsymbol{i}}$. The second step filters the remaining dense reconstruction points by applying a threshold of the directional difference of the computed PMVS patch surface normals from the estimated parking lot surface normal. The threshold value of $|20°|$ was determined experimentally. This procedure reduced the RMS error between $\hat{\boldsymbol{L}}_{\boldsymbol{i}}{}'$ and $\hat{\boldsymbol{L}}_{\boldsymbol{i}}$ to within 0.3m under most cases, which has proven thus far to provide sufficient alignment for robust classification.

D. Classification

A classifier was designed based on estimating the above-plane 3D point probabilities within each parking space with respect to the total number of reconstructed 3D points. The estimate is computed by segmenting and summing the above-plane points which lie within a 6-sided convex 3D polyhedron, defined by intersecting 4 vertical planes aligned with the vertical Z-axis and coincident with the parking lanes and their front/back end points, and a horizontal plane elevated 5 meters above the parking lot surface (US regulation height for semi-tractor trailers is 4.15m). Based on empirical observation, a cut-off of 0.2 meters above the parking lot surface was selected to filter above-plane parking lot surface points from the parking lot plane (Fig. 2). The 3D point probabilities associated with ground truth observations are then used to determine an optimal decision boundary for occupancy which minimized type I (False Positives) and type II (False Negatives) errors using a Golden Search algorithm.

An initial set of 21,588 parking observations collected in the first half of 2013 was used as a training set to build the classifier $(6 \text{ spaces} \times 3,598 \text{ samples})$. The collected data expressed variations in parking behaviors, vehicles, environmental conditions and, seasonal weather, during both day time (51.8%) vs. night time (48.2%) periods. An optimal decision ratio boundary of 0.0075 yielded a total error rate of 2.2%, which corresponds to a detection accuracy = $100\% \times (1-(FN+FP)/N) = 100\% \times (1-(326+137)/21,588) = 97.8\%$.

III. SYSTEM DESIGN AND IMPLEMENTATION

A detection system (Fig. 4) has been deployed at a state sponsored rest area which is accessible to west bound traffic on a major interstate highway approximately 25 miles west of Twin Cities in Minnesota. The truck parking facilities design consists of a single row of 15 dedicated parking spaces, 4.26m wide and 26.0m in length. Three camera poles were placed along the perimeter of the parking facilities between 14.7 and 9.1 meters from the front boundary of the parking spaces. Each pole can support the multi-view SfM algorithm by allowing up to three commercial Off-The-Shelf (COTS) HD 1920x1090 PTZ network cameras to be mounted across a horizontal bar providing an end-to-end 4.2 meter baseline at the top of 10.7 meter (35 ft.) crank-down poles.

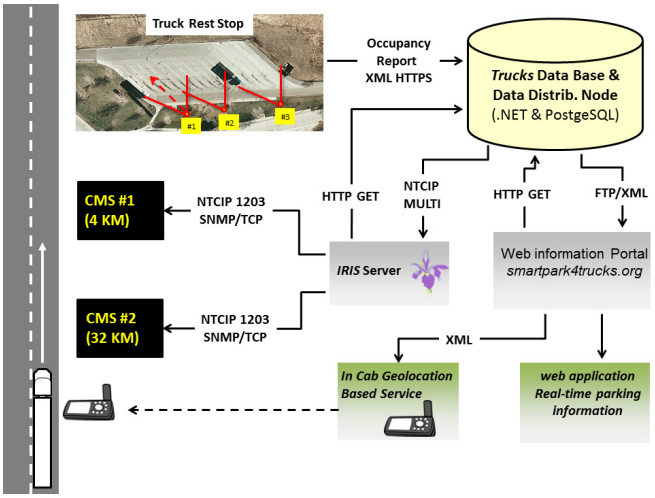

Fig. 4: System design.

For this specific site configuration, about 5 to 6 spaces can

be captured simultaneously by overlapping three PTZ cameras such that their focal centers are approximately aligned with a 55° horizontal field of view. The aforementioned algorithm is implemented on a desktop PC with an Intel i7 3770K 3.5Ghz Quad-core processor running Linux kernel 3.2.0-23. PC and communication hardware reside within the visitor shelter of the rest area. Below grade conduit carries power and commutations from the shelter to each crank-down camera pole.

Real-time count and occupancy data for the site are uploaded to a relational database, and web-based data distribution server (DDS). The DDS records the reception time and stores the report in a relational database. The data is also disseminated to three different information portal systems: 1. Web-based information dissemination portal, 2. In-cab services, and 3. Roadside Changeable Message Signs via an XML feed queried with the RESTful interface or an FTP connection. An Intelligent Roadway Information System server (IRIS) [23] queries the DDS to communicate with roadside Variable Message Signs using a standardized (NTCIP) communication protocol [24].

IV. RESULTS

In order to investigate the persistence in detection accuracy for this study, historical data were harvested.at either 2 or 5 minute intervals over the course of 96 hours during late summer (August 2013). The parking state for each observed parking space in the sets of data were manually labeled. Note that other observed phenomena that may affect detection or the observation were also categorized as: 1) vehicles double-parked/encroaching onto an adjacent lane, 2) parking space utilization from a non-commercial heavy vehicle 3) observable environmental conditions, 4) camera obstructions, and 5) truck maneuvers, such as pulling in, or pulling out of the space.

TABLE I: Hourly Occupancy Detection Performance

Hour	Sensitivity	Specificity	Accuracy	Samples
0	98.77%	97.83%	98.61%	1867
1	97.89%	96.14%	97.65%	1872
2	97.39%	98.86%	97.60%	1872
3	97.34%	99.31%	97.65%	1872
4	97.16%	98.04%	97.33%	1872
5	98.88%	99.09%	98.93%	1872
6	99.42%	99.85%	99.57%	1872
7	99.56%	100.00%	99.79%	1872
8	99.56%	99.69%	99.63%	1872
9	99.13%	100.00%	99.66%	1782
10	99.03%	99.91%	99.59%	1692
11	99.32%	100.00%	99.77%	1712
12	97.91%	99.92%	99.30%	1715
13	99.33%	99.73%	99.64%	1928
14	98.94%	99.94%	99.68%	2202
15	97.81%	99.66%	99.19%	2342
16	99.39%	99.16%	99.24%	2370
17	99.39%	98.92%	99.11%	2370
18	99.72%	99.77%	99.75%	2370
19	99.88%	99.81%	99.84%	1872
20	98.71%	98.31%	98.50%	1872
21	98.74%	98.53%	98.66%	1867
22	98.95%	98.53%	98.83%	1877
23	98.33%	98.42%	98.34%	1872

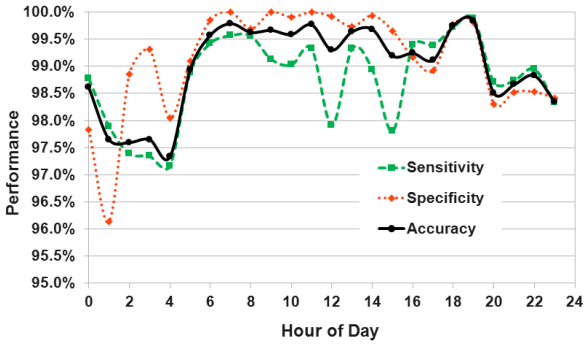

Fig. 5: Performance by time of day (local-time).

For the August 2013 data, the individual ground truth tables for each parking space indicate an overall detection accuracy of 99.01%, with the lowest accuracy equal to 95.93% and the highest accuracy equal to 100.0%. Over 95.3% of the samples produced correct occupancy classifications, while 4.29% had one incorrect occupancy classification and the remaining 0.31% had two or more incorrect classifications. In Table II, specificity refers to the true parking space occupancy detection rate calculated by $100\% \times (TP/(TP+FN))$ and sensitivity refers to the space vacancy detection rate calculated by $100\% \times (TN/(TN+FP))$. Similar to the training set, sensitivity trended lower than specificity. Despite these errors, the level of accuracy demonstrates a persistent high level of performance for detection and classification. Fig. 5 illustrates time-of-day performance trends for all 15 parking spaces, by aggregating the data into 1 hour bins (Table I). Daylight hours (6:00 AM - 8:00 PM) had an average accuracy of 99.51% while night hours had an average accuracy of 98.36%. Note that the proportions of day time and night time observations were 57% and 43% respectively. Analysis of the miss-classification indicates that typical sources of error include: edge cases of ground truth such as when vehicles are pulling in or out of the space, double parking cases where slight encroachments of vehicles crossing over the lane line were observed, and low light conditions with dark colored vehicles which resulted in inaccurate 3D reconstruction and coordinate system realignment. Low light induced miss-classification could be improved by additional on-site lighting.

V. CONCLUSIONS

The efficacy of a novel sensing method was presented that leverages recent advances in 3D SfM techniques to extract truck parking occupancy from adjacent multiple camera views of the scene. This differs from other computer vision approaches found in literature to address parking occupancy detection. The method is robust in snowy weather and under various lighting conditions. It is able to detect a variety of vehicles including different truck types and passenger cars. With this technique, the same group of cameras can also be used to capture several overlapping regions of the lot to reconstruct several parking spaces, thereby leveraging economies of scale for such a system. Longer term field

TABLE II: Occupancy Detection Performance

Lane	1	2	3	4	5	6	7	8
FN	14	13	10	4	7	0	10	7
FP	27	1	4	7	2	0	3	7
TN	1482	1321	1018	1315	1303	1175	1709	1411
TP	1590	1778	2081	1787	1801	1938	1440	1737
Total	3113	3113	3113	3113	3113	3113	3162	3162
Sensitivity	99.13%	99.27%	99.52%	99.78%	99.61%	100.00%	99.31%	99.60%
Specificity	98.21%	99.92%	99.61%	99.47%	99.85%	100.00%	99.82%	99.51%
Accuracy	98.68%	99.55%	99.55%	99.65%	99.71%	100.00%	99.59%	99.56%
Frequency of Occupation	51.53%	57.53%	67.17%	57.53%	58.08%	62.26%	45.86%	55.15%

Lane	9	10	11	12	13	14	15		Total Result
FN	3	0	118	122	9	19	5		341
FP	8	48	0	3	5	5	3		123
TN	1659	2030	1802	1340	1812	1757	430		21564
TP	1492	1084	1152	1607	1246	1291	2634		24658
Total	3162	3162	3072	3072	3072	3072	3072		46686
Sensitivity	99.80%	100.00%	90.71%	92.94%	99.28%	98.55%	99.81%		98.64%
Specificity	99.52%	97.69%	100.00%	99.78%	99.72%	99.72%	99.31%		99.43%
Accuracy	99.65%	98.48%	96.16%	95.93%	99.54%	99.22%	99.74%		99.01%
Frequency of Occupation	47.28%	34.28%	41.34%	56.28%	40.85%	42.64%	85.90%		53.55%

studies regarding the efficacy of this technology will be done with additional rest area installations in order to more fully assess long term performance and refine it. Future plans are to expand the system to several more rest areas along an Interstate highway corridor as part of a region-wide, real-time truck parking information system as well as gather detailed long-term historical information on parking utilization.

ACKNOWLEDGMENT

The authors acknowledge former graduate student Eric Holec, and students associated with the Center for Distributed Robotics, Department of Computer Science, for their diligent and thoughtful assistance with the classification process.

REFERENCES

[1] S. L. Hallmark, Y.-Y. Hsu, T. Maze, T. McDonald, and E. Fitzsimmons, "Investigating factors contributing to large truck lane departure crashes using the federal motor carrier safety administrations large truck crash causation study (ltccs) database," USDOT Volpe, Cambridge, Massachusetts, Tech. Rep. SS-90/01, Jan. 2009.

[2] T. L. Bunn, S. Slavova, T. W. Struttmann, and S. R. Browning, "Sleepiness/fatigue and distraction/inattention as factors for fatal versus nonfatal commercial motor vehicle driver injuries," *Accident Analysis and Prevention*, no. 37, pp. 862–869, 2005.

[3] T. Sando, M. Angel, E. Mtoi, and R. Moses, "Analysis of the relationship between operator cumulative driving hours and involvement in preventable collisions," in *90th Annual Meeting of the Transportation Research Board*, Washington, D.C., Jan. 2011.

[4] S. W. Park and P. P. Jovanis, "Hours of service and truck crash risk: Findings from 3 national us carriers during 2004," *Journal of the Transportation Research Board*, no. 2194, pp. 3–10, 2010.

[5] K. G. Scott B. Smith, W. Baron and G. Ritter, "Intelligent transportation systems and truck parking," USDOT Federal Motor Carrier Safety Administration (FMCSA), Washington D.C., Tech. Rep. FMCSA-RT-05-001, Feb. 2005.

[6] J. W. Trombley, "Dealing with truck parking demands," Transportation Research Board, National Cooperative Highway Research Program, Washington D.C., Tech. Rep. Synthesis (NCHRP) 317, 2003.

[7] J. Fallon and K. Howard, "Smartpark truck parking availability system: Magnetometer technology field operational test results," Federal Motor Carrier Safety Administration, Washington D.C., Tech. Rep., Jan. 2011.

[8] J. Gertler and J. Murray, "Smartpark truck parking availability system: Video technology field operational test results," Federal Motor Carrier Safety Administration, Washington D.C., Tech. Rep., Jan. 2011.

[9] P. Modi, V. Morellas, and N. Papanikolopoulos, "Counting empty parking spots at truck stops using computer vision, final report," ITS Institute, Minneapolis, Minnesota, Tech. Rep. CTS 11-08, May 2011.

[10] Q. Wu, C. Huang, S. Wang, W.-C. Chiu, and T. Chen, "Robust parking space detection considering inter-space correlation," in *2007 IEEE International Conference on Multimedia and Expo*, Beijing, China, 2007, pp. 659–662.

[11] N. True, "Vacant parking space detection in static images," University of California, San Diego, San Diego,CA, May 2007.

[12] Y.-W. Seo and C. Urmson, "Utilizing prior information to enhance self-supervised aerial image analysis for extracting parking lot structures," in *the 2009 IEEE/RSJ International Conference on Intelligent Robots and Systems*, St. Louis, Missouri, Oct. 2009, pp. 339–344.

[13] D. B. L. Bong, K. Ting, and N. Rajaee, "Car-park occupancy information system," in *3rd Real-Time Technology And Applications Symposium*, Dewan Taklimat, Malaysia, Dec. 2006.

[14] H. Deng, D. Jiang, and Y. Wei, "Parking cell detection of multiple video featrues with pca-and-bayes-based classifier," in *Proc. of the 2006 IEEE Internation Conference on Information Acquisition*, Weihai, Shandong, China, Aug. 2006, pp. 655–659.

[15] H. R. H. Al-Absi, J. D. D. Devaraj, P. Sebastian, and Y. V. Voon, "Vision-based automated parking system," in *10th International Conference on Information Science, Signal Processing and their Applications, ISSPA*, Kuala Lumpur, Malaysia, May 2010, pp. 767–760.

[16] D. J. Cook, "Parking space occupancy detection utilizing 3D reconstruction techniques," Master's thesis, University of Minnesota, Minneapolis, MN, 2012.

[17] T. Morris, "Error analysis of six degree of freedom tracking systems," Master's thesis, University of Minnesota, Minneapolis, MN, 1989.

[18] Y. Furukawa and J. Ponce, "Accurate, dense, and robust multi-view stereopsis," *IEEE Transactions on Pattern Analysis and Machine Intelligence*, vol. 32, no. 8, pp. 1362–1376, 2010.

[19] N. Snavely, S. M. Seitz, and R. Szeliski, "Photo tourism: Exploring photo collections in 3D," in *ACM Transactions on Graphics*, 2006, pp. 835–846.

[20] D. G. Lowe, "Distinctive image features from scale-invariant keypoints," *Journal of Computer Vision*, vol. 60, no. 2, pp. 91–110, 2004.

[21] M. Lourakis and A. Argyros, "Sba: A software package for generic sparse bundle adjustment," *ACM Trans. Mathmatics Software*, vol. 36, no. 1, pp. 1–30, 2009.

[22] G. H. Schut, "On exact linear equations for the computation of the rotation elements of absolute orientation," *Photogrammetria*, vol. 17, no. 1, pp. 34–37, 1961.

[23] (2013) "Intelligent Roadway Information System". [Online]. Available: http://iris.dot.state.mn.us/

[24] "National transportation communications for its protocol object definitions for dynamic message signs (dms)," AASHTO, ITE, NEMA, Washington D.C., Tech. Rep. 1203 v03-04 Part 1 dms2011, May 2011.